Articles in PresS. J Neurophysiol (June 22, 2011). doi:10.1152/jn.00995.2010

NEURAL CORRELATES OF COGNITIVE CONTROL OF REACHING MOVEMENTS IN THE DORSAL PREMOTOR CORTEX OF RHESUS MONKEYS

***G. Mirabella[1,3], P. Pani[1,2], S. Ferraina[1]**

[1]Department of Physiology and Pharmacology and [2]PhD Program in Neurophysiology, Sapienza University of Rome; [3]Department of Experimental Medicine, University of L'Aquila

Running head: *Neural mechanisms of reaching movements inhibition*

- Number of figures and tables 8 and 2
- Number of pages (Main Text without References) 33
- Number of words for Abstract: 153 words

Keywords: countermanding task; voluntary control; dorsal premotor cortex; reaching movements

Acknowledgments: Supported by MIUR (grant n.2005051741 to SF) and by the Italian National Institute of Health (grant n. 530/F4/1 to SF). We are grateful to M Mattia and P Del Giudice for invaluable comments on a previous version of the manuscript, to R Caminiti for support throughout this research and to AR Mitz for advice concerning the Cortex set-up. Mirabella wishes to thank the Head of the Department of Physiology and Pharmacology of Sapienza University, F Eusebi, for his support advice and encouragement during the preparation of the manuscript.

Pierpaolo Pani current address: Lab Neuro- en Psychopysiologie, K.U. Leuven, Medical School, Campus Gasthuisberg, Herestraat 49, B-3000, Leuven, Belgium

Corresponding authors:

Prof. Stefano Ferraina
Department of Physiology and Pharmacology
Sapienza University
Piazzale Aldo Moro 5, 00185 Rome, Italy
ph: +39 06 4991 0306; fax: +39 06 4969 0236
e-mail: stefano.ferraina@uniroma1.it

Giovanni Mirabella, PhD

Department of Experimental Medicine
University of L'Aquila
via Vetoio, Coppito Due,67100 L'Aquila, Italy
ph +39 06 4991 2312 ; fax +39 06 4991 0860
e-mail: giovanni.mirabella@uniroma1.it

ABSTRACT

Cancelling a pending movement is a hallmark of voluntary behavioural control because it allows to quickly adapt to unattended changes either in the external environment or in our thoughts. The countermanding paradigm allows to study inhibitory processes of motor acts by requiring to withhold planned movements in response to an infrequent stop signal. At present the neural processes underlying the inhibitory control of arm movements are mostly unknown. We recorded the activity of single units in the rostral and caudal portion of the dorsal premotor cortex (PMd) of monkeys trained in a countermanding reaching task. We found that among neurons with a movement-preparatory activity, about one third exhibits a modulation before the behavioral estimate of the time it takes to cancel a planned movement. Hence these neurons exhibit a pattern of activity suggesting that PMd plays a critical role in the brain networks involved in the control of arm movement initiation and suppression.

Introduction

Living in a world where events cannot be predicted with certainty, the ability of suppressing a pending action after unexpected changes in the environment or in our mind is fundamental. In these instances, volitional inhibition plays a key role in the control of behaviour, preventing the prepared movement from occurring. This form of inhibitory control has been studied quantitatively using the countermanding paradigm (Logan 1994). The paradigm probes a subject's ability to withhold a planned movement triggered by a go signal when an infrequent stop signal is presented after a variable delay. The behavioural performance of the countermanding task has been modelled by Logan and Cowan (1984) and allows the estimation of an otherwise unobservable variable: the time it takes to cancel a planned movement, the 'stop signal reaction time' (SSRT; Band et al. 2003; Boucher et al. 2007; Logan and Cowan 1984).

During the past 15 years, neural substrates of movement suppression were explored by correlating the behavioural performance in the countermanding task either with the modulation of neural activity in monkeys (Hanes et al. 1998; Ito et al. 2003; Stuphorn et al. 2000; Paré and Hanes 2003), or fMRI's BOLD activity in volunteers (Aron and Poldrack 2006; Li et al. 2008) or with localized brain lesions in patients (Aron et al. 2003). In particular, single unit studies revealed that the frontal eye field (FEF; Hanes et al. 1998) and the superior colliculus (SC; Paré and Hanes, 2003) contain neurons with activity patterns sufficient to control saccade cancellation. In both studies eye movements' suppression is typically associated with a decrease of activity of movement related neurons before the end of the SSRT and a simultaneous increase of activity in neurons controlling fixation.

Arm movements, differently from saccades, are those that allow physical interactions with the environment, thus leading to obtain material outcomes, such as the grasping of food, and not only to obtain emotional rewards. So far little is known about the neural processes underlying the inhibitory control of manual movements.

In humans, evidence from lesion (Aron et al. 2003), neuroimaging (Rubia et al. 2003), and transcranial magnetic stimulation (TMS; Chambers et al. 2006) studies, where subjects were required to execute/inhibit a key-press, show the involvement of right inferior frontal cortex (IFC) in the executive control of motor suppression. Aron et al. (2006) and Li et al. (2008) suggested, respectively, that prefrontal cortex countermands planned movements through the right subthalamic nucleus and the head of the caudate nucleus. These brain regions are likely, in turn, exerting their action influencing the primary motor cortex (M1) and the dorsal premotor area (PMd), i.e., those cortical areas critically involved in limb movement preparation and initiation (Cheney and Fetz 1980; Churchland et al. 2006; Churchland and Shenoy 2007; Evarts 1968; Riehle and Requin 1993; Thach 1975; Weinrich et al. 1984). In line with this hypothesis Coxon et al (2006) by applying the TMS on M1 during the execution of a countermanding task demonstrated that this area plays a key role in movement cancellation. Epicortical EEG recordings signals, further confirmed this evidence (Swann et al. 2009).

In monkeys, recordings of neural activity during Go/No-Go tasks, showed the involvement in movement suppression of both M1 (Miller et al. 1992; Port et al. 2001) and PMd (Kalaska and Crammond 1995). However in the Go/No-Go paradigms it is a potential movement and not an ongoing response that has to be halted. To date the only study in which activity of single neurons were recorded during a manual version of the

countermanding task, it is the one of Scangos and Stuphorn (2010). They recorded from the supplementary motor area (SMA) and pre-SMA of monkeys, and they found that the activity of these regions does not control arm movement initiation, but might contribute to movement suppression. The latter conclusion has been confirmed by Chen et al (2010), who showed that local fields potentials (LFPs) power spectra obtained from data recorded over SMA, display changes in the low frequency range (10-50 Hz) early enough to suggest that this region is causally involved in movement inhibition. However, it has to be stressed that the percentage of neurons causally involved in movement suppression found by Scangos and Stuphorn (2010) was rather small, i.e., only 8 neurons out of 335 (2.4%). Even though it could not be excluded the presence of a recording bias or other factors that might have influenced the total number of identified neurons, it is also plausible to hypothesize that SMA and pre-SMA are not the main actors in cancelling a movement after the appearance of an imperative stop signal. This interpretation is not in contrast with the finding of Chen et al (2010) because changes in LFPs could be caused not by the local activity but by inputs coming from other brain regions (Logothetis, 2003; Mattia et al 2010).

In the present study, we have reinvestigated the neural correlates of volitional cancellation of a pending arm movement, by recording the responses of area PMd neurons in two monkeys performing a countermanding reaching task. For the first time, we report the existence in PMd of reaching-related neurons showing a modulation of activity related to the suppression of programmed arm movements.

METHODS

Surgical Techniques

Two adult male rhesus macaques (*Macaca mulatta; monkey S and monkey L*) weighing 7-8 Kg were used. Before starting the training, under aseptic surgical conditions, a head holding device, and a scleral eye coil (Robinson 1963) were implanted. Antibiotics and analgesics were administered postoperatively. In each monkey, at the end of the training period, again under general anesthesia, a recording cylinder (18 mm in diameter) was implanted stereotaxically in the left frontal lobe in order to allow recordings over the arm representation of the PMd (Paxinos et al. 2000). The location of the neural recordings was confirmed by structural MRI on monkey S and visual inspections of the anatomical landmarks, such as the central (CS) and the arcuate sulcus (AS), on monkey L, after opening the dura. Both animals have been sacrificed at the end of the experimental procedures. In the present paper we will deal only with recordings obtained from PMd (Figure 1A).

Animal care, housing, and surgical procedures were in conformity with the European (Directive 86/609/ECC) and Italian (D.L. 116/92) laws on the use of nonhuman primates in scientific research.

Apparatus and electrophysiological recordings

Animals were placed in a darkened, sound attenuated chamber and seated in a primate chair, with their head fixed in front of 21" PC monitor (CRT non interlaced, refresh rate 85 Hz, 800x600 resolution, 32 bit color depth; distance monitor-eye: 21 cm), equipped with a touch screen (MicroTouch, sampling rate 200Hz) for touch positions monitoring.

153 Touch screen sensitivity was set to the maximum value in order to detect minimal
154 changes in the touch position. A non commercial software package, CORTEX
155 (www.cortex.salk.edu), was used to control stimuli presentation, behavioral responses
156 and to collect neural (1000 Hz) and eye-movement (200 Hz) data. During the task, eye
157 movements were monitored by using a magnetic search coil technique (Fuchs and
158 Robinson 1966; Remmel labs, Ashland, MA). Saccades were detected off-line using
159 velocity threshold criteria (30 deg/s). Eye's reaction times were measured as the interval
160 from target appearance to the beginning of the saccade.

161 Neural activity of single units was recorded extracellularly using a seven channel
162 multielectrode system (Thomas Recording, Giessen, Germany). Electrodes were quartz-
163 insulated platinum-tungsten fibers (80 μm diameter, 0.8-2.5 MΩ impedance) and were
164 inserted transdurally, one at a time, using microdrives (Thomas Recording, Giessen,
165 Germany). Electrical signals were amplified, filtered, and single unit were isolated on-
166 line exploiting a dual time amplitude window discriminator (BAK electronics, Mount
167 Airy, MD).

168

169 ***Stimuli, task and neuron selection***

170 Visual stimuli consisted of red circles (2.43 cd/m^2) with a diameter of 7.6° (2.8 cm) on a
171 dark background of uniform luminance (<0.01 cd/m^2). The presentations of the stimuli
172 were synchronized with the monitor refresh rate (85 Hz). Monkeys were required to use
173 the arm (right arm) controlateral to the recording hemisphere. The other arm was
174 physically constrained.

After one or two cells were isolated at each electrode, we qualitatively determined if neurons exhibited a preparatory activity correlated to reaching movements with an instructed delay task (Johnson et al. 1996). The delay task allowed us to qualitative select neurons showing preparatory activity. Whenever we had at least four isolated neurons with preparatory activity across all electrodes, a reaching version of the countermanding task was administered (see Figure1B; Mirabella et al. 2006; Mirabella et al. 2008; Mirabella et al. 2009). It consisted of one block of 480 trials, where no-stop trials (67%) were randomly intermixed with stop trials (33%). All trials began with the appearance of a stimulus at the center of the display (Figure 1B). Monkeys were required to touch it with their finger/s, within 2 s, and hold it for 500-800 ms. In the *no-stop trials* the central stimulus went off and, simultaneously, a target appeared (go-signal) randomly at one of two possible opposite positions, 21.8° (8 cm) from the central stimulus, virtually arranged in a circle at 45° of interval between the potential positions. For each trial, targets were presented at the preferred location (corresponding to the positions that better modulated most of the isolated neurons) or at the opposite one. To get the juice reward, animals were required to reach and hold the target for 300 ms. *Stop trials* differed from the no-stop trials because at a random delay (stop signal delay, SSD), during the reaction time (RT), the central stimulus reappeared. In these instances, monkeys had to inhibit the pending movements, holding the central position for an additional interval of 650-850 ms (450-550 ms for monkey L) after stop appearance, until reward delivery. To discourage monkeys from adopting the strategy of slowing down RT for maximizing the number of correct responses to stop signals we set a maximum time for response, named upper RT

197 (600 ms for monkey L; 750 ms for monkey S). An auditory feedback was given for
198 correct responses. A time-out of 800 ms was given after each error.

199 The probability of inhibiting a movement critically depends on the length of the
200 SSD. Stopping becomes increasingly more difficult as the SSD is lengthened. Logan and
201 Cowan (1984) developed the horse-race model to explain these results. The model
202 assumes that the behavioral outcome of the task is the result of a race (Figure 2A)
203 between two stochastically independent processes: a go process triggered by the go
204 stimulus and a stop process triggered by the stop signal. If the stop process wins,
205 participants will inhibit their response (success). On the other hand, when the go process
206 wins, participants will respond (failure). Recently, the assumption of independence of
207 the two processes had been challenged. Boucher et al (2007) proposed an interactive race
208 model, in which the go and stop processes are independent for much of their latencies but
209 interact near the end of the race, when the stop process tries to interrupt the go process.
210 However even in the new formulation the model reliably describes the performance in the
211 countermanding task and allows the estimation of the SSRT.

212 In the two animals, we used two different procedures for setting the SSDs. In most
213 sessions (all 33 sessions for monkey L and 9 out of 24 sessions for monkey S) we used a
214 *fixed-SSD procedure* (Band et al 2003). On the basis of the average RT measured at the
215 beginning of each session, we computed four progressively longer SSDs so that monkeys
216 were able to successfully inhibited a movement in ~85%, ~65%, ~35% and ~15% of the
217 stop trials. The SSDs were set independently for each of the two movement directions, to
218 compensate for possible differences of RT. Whenever, after some trials, we realized that
219 the performance did not satisfy the above defined criteria, the SSDs were adjusted and

the session was restarted until a good control of the behaviour was obtained for at least one of the two directions of movement. In monkey L the SSDs ranged from 129.4 ms (11 units of refresh rate) and 341 ms (29 units of refresh rate), with a mean value of 219.7 ± 4.16 ms (variance will always be reported with the standard error). In monkey S the SSDs ranged from 117.6 ms (10 units of refresh rate) and 471 ms (40 units of refresh rate), with a mean of 341.1 ± 14.5 ms.

In 15 experimental sessions of monkey S, the length of the SSDs were dynamically changed using a *staircase procedure* (Band et al. 2003; Mirabella et al. 2008; Mirabella et al. 2009; Osman et al. 1986; Osman et al. 1990). The SSD duration varied from one stop trial to the next according to the behavioral performance: if the monkey succeeded in withholding the response, the SSD increased by 5 refresh rates (or 58.8 ms), if it failed, the SSD decreased by the same amount of time. We used two independent staircases, one for each movement direction, to compensate for eventual differences in RT. Both staircases started from a SSD of 246.9 ms (21 refresh rates), which preliminary data obtained in monkey S, suggested were appropriate for quickly obtaining the desired performance (50% success). This procedure provides different SSDs for each sessions, however, to maintain a similar statistical power we had for the fixed-SSD procedure, we further analyzed the neural responses only when a SSD was presented at least 20 times and when at least 5 of these trials were correctly suppressed.

Behavioral analysis

Since in each session the target could appear at two possible locations, from each countermanding block we obtained either two inhibition functions (that is the relationship

between the probability of stop-failure trial occurrence as a function of the SSDs), one for each target direction, or two possible outcomes of the staircase procedures. To derive reliable parameter estimates for each inhibition function, the data were fit with a Weibull cumulative distribution ($W(t)$, where t is time after target presentation; Hanes et al 1998). Overall, the Weibull function fits had a mean r^2 of 0.8 (±0.02) and the χ^2-test was always non significant (ps>0.05). For each inhibition function, we estimated the SSRT using the two methods described in detail in Mirabella et al (2006), based on two different assumptions. The first method assumes that SSRT is a random variable. Under this hypothesis the SSRT is estimated by the difference between the mean RT of no-stop trials and the mean of inhibition function (method of the mean; Logan and Cowan 1984; Hanes and Schall 1995). The mean of the inhibition function corresponds to the SSD at which p(failure) = 0.5. We evaluated numerically the integral using the fitted $W(t)$ and a trapezoidal rule with bins of 1 ms (Hanes et al. 1998):

$$\overline{SSRT} = \overline{RT} - \int_{-\infty}^{+\infty} t \frac{dW(t)}{dt} dt$$

The second method assumes that the SSRT is a constant and that go process durations are roughly the same for no-stop and stop trials (integration method; Band et al. 2003; Logan and Cowan 1984). Using this method, the SSRT is obtained for each given SSD, by subtracting the finishing time of the stop process from the starting time (the SSD value). The finishing time of the stop process is calculated by integrating the no-stop trials RT distribution from the onset of the go-signal until the integral equals the corresponding observed proportion of stop-failure trials (Logan 1994). Then the SSRT is calculated as the mean value of the SSRT computed at each SSD.

Whenever the staircase procedure was employed, the SSRT was computed using two procedures (described in details in Mirabella et al 2009), both based on the use of the integration method. The two procedures differed for the method used to obtain the starting time. In the first procedure, for each session, using the mid-run estimate method (Levitt 1971; Wetherill and Levitt 1965; Wetherill 1966), we worked out the starting time as the delay that better corresponds to the time needed to the subject to withhold a response about 50% of the times ('representative' SSD). In the second procedure, for each session, we took as starting times the length of those SSDs that were presented at least 20 times. For each SSD selected a value of the SSRT was computed, then the behavioral estimate of cancellation time in a given session was obtained by averaging all the SSRTs computed at each SSD.

In summary, whatever the method used for setting the SSDs (fixed or staircase), we obtained, for each recording session, two estimates of the SSRT for each direction of movement/target appearance.

Neuronal data analysis

Whenever not differently specified, for each neuron with a significant preparatory activity (see Results), we analyzed neural data for the movement direction for which we had the best behavioral performance. That is, as for as the fixed-SSD procedure is concerned, we selected the movement direction for which inhibition function was as close as possible to the one desired, i.e., the one for which the monkeys failed to successfully cancel a movement in ~15% (shortest SSD), ~35% (2^{nd} SSD), ~65% (3^{rd} SSD), ~85% (longest SSD) of the stop trials. For the *staircase procedure* we considered

288 the movement direction for which the p(failure) was closest to 0.5. In both cases, only
289 data from one direction of movement have been used to assess for countermanding
290 related modulations.

291 To visualize the neural data, rasters of neuronal discharge and spike density
292 functions were aligned on the time of the go-signal. Spike density functions were
293 obtained by convolving spike trains with Gaussian kernel function (kernel width 13 ms).

294 To detect countermanding related activity in our sample of neurons, following the
295 line of reasoning of Hanes et al (1998) and of Paré and Hanes (2003), we contrasted the
296 activity during stop-success trials with the activity recorded during those no-stop trials in
297 which the reaching movement initiation would have been canceled if the stop signal had
298 been presented at the same SSD. These are the trials in which, given the length of the
299 SSRT, the go-process was slower than the stop-process if the stop signal had occurred.
300 This subset of no-stop trials, which we will refer to as *latency matched no-stop trials*, is
301 given by those reaching movements with RTs greater than the sum of the SSD and the
302 SSRT calculated from the same data (e.g., for the longest SSD, dark region of the no-stop
303 trials RT distribution in Figure 2B). To quantify the time course of the neuronal
304 activation during stop-success trials and latency matched no-stop trials, we calculated a
305 *differential spike density function* (Hanes et al. 1998) by subtracting the absolute values
306 of the average spike density functions (aligned on the time of the go-signal) associated
307 with each type of trials. We defined the time at which significant differential activation
308 began (and we named it the *neural cancellation time*) as the instant when the differential
309 spike density function exceeded at least by 2 SD the mean value of the differential
310 activity recorded during the 300 ms period preceding the go signal provided that the

311 difference remained above this threshold for at least 60 ms. The reference period was
312 subdivided in 12 bins (each lasting 25 ms), neural activity was calculated for each bin in
313 absolute value and finally the mean and SD values across bins were worked out.
314
315

RESULTS

Behavioral estimate of reaching arm movements cancellation

To control in our data the validity of the stochastic independence of go and stop processes, we checked how well the race model predicted the RTs of stop-failure trials, that is the RTs of those reaching movements that could not be cancelled even though a stop signal was presented (Logan and Cowan 1984; Mirabella et al 2006; Mirabella et al 2008). In stop-failure trials, reaching movements were produced because the go process won the race against the stop process. Therefore, considering the distribution of the RTs of the no-stop trials, the responses that would not be stopped despite the presentation of the stop signal should be those corresponding to reaching movements with RTs shorter than the SSD plus the SSRT (e.g., for the longest SSD, light region of the no-stop trials RT distribution in Figure 2B). Three predictions should be satisfied (Logan and Cowan 1984; Logan 1994). First, the mean RT in stop-failure trials should never be longer than the mean RT in the no-stop trials. Second, the mean RT in stop-failures trials should linearly increase with increasing SSDs. Third, the mean RT in the stop-failure trials at each SSD should be equal to those predicted from the race model. Figure 3 shows that in an example session these predictions were satisfied. Figure 3A shows that the cumulative RT distribution for no-stop trials (mean 285.8 ± 3.1 ms) is shifted to the right with respect to the cumulative RTs distribution of stop-failure trials (mean 268.4 ± 4.2 ms), namely the latter are faster than the former (Kolmogorov-Smirnov test; $p<0.0005$). From the same dataset, Figure 3B shows that the second and the third prediction of the race model are also satisfied. In fact RTs in the stop-failure trials increase as a function of the length of the SSDs and that they are not significantly different from those predicted by the race

339 model (paired t-test; ps>0.05), with the known exception of the shortest SSD (Logan
340 1994). All these predictions were largely satisfied across all sessions in both monkeys.
341 The RTs in stop-failure trials were significantly shorter than the RTs in the no-stop trials
342 (see Table 1; Kolmogorov-Smirnov test; p*s*<0.05) in 45/54 cases (or 83.3%). The other
343 two assumptions were tested in those sessions were the fixed-SSD procedure was
344 employed. Linear regression analysis showed that in all occurrences but 2 (40/42 or
345 95.2%) the mean RTs in stop-failures trials increases with increasing SSD (mean slope
346 0.56 ± 0.08). The violations observed for the shortest SSD are consistent with previous
347 observations, and they are attributed either to the very few stop-failure trials occurring at
348 the shortest SSD (Logan and Cowan 1984; Logan 1994; Mirabella et al 2006) or to self-
349 generated movements produced after the initial movement was inhibited (Boucher et al
350 2007). Finally, in the 125 out of 154 cases (or 81.1 %) the observed mean RTs in the
351 stop-failure trials at each SSD were equal to those predicted (t test, ps>0.05).
352 Figure 4A plots the inhibition function, and the corresponding $W(t)$, for one
353 representative session of monkey L. Figure 4B shows the average inhibition function
354 across all sessions separately for the two monkeys. To obtain the latter, data from single
355 sessions were combined by averaging for each single SSD the probability of generating a
356 movement [p(failure)], even though a stop signal was presented. These results
357 demonstrate the reliability of the behavioural control. In the staircase sessions the
358 goodness of the behavioral control was further witnessed by the fact that the average
359 p(failure) was close to 0.5 (0.48 ± 0.3; Table 1; see also Band et al. 2003).
360 Table 1 summarizes all relevant parameters describing the behavioral
361 performance of each monkey for all sessions used for the analysis of the neural activity,

362 separately for the fixed-SSD procedure and the staircase procedure. Using the fixed SSD
363 procedure, the SSRT estimated with the integration method did not significantly differ
364 from that obtained assuming that the SSRT is a random variable (paired t-test; monkey L:
365 df=32, t=0.97, p = 0.34; monkey S: df=8, t=-1.1, p=0.29). Therefore, we averaged them
366 (monkey L: average SSRT = 137.7 ms; monkey S: average SSRT = 160.6 ms). In
367 monkey S, two other estimates of the SSRT were obtained from the analysis of the
368 staircase sessions. Again, the two estimates of the SSRT were not significantly different
369 (paired t-test, df=14, t=0.001, p=0.99), thus, we averaged them (average SSRT = 147.5
370 ms). These values of SSRT for reaching arm movements are very similar to those
371 recently reported (about 140 ms) by Scangos and Stuphorn (2010) for arm movement in
372 monkeys.
373
374 ***Classification of neural activity***
375 A total of 163 individual neurons were recorded from the left PMd areas of the two
376 monkeys (93 and 70 neurons from monkey L and S, respectively).
377 As a first step we assessed the number of cells exhibiting a reaching related
378 activity in the selected direction (on the basis of the good behavioral control; see
379 Methods). To this end, for each recorded cell, we compared with an analysis of variance
380 (one-way-ANOVA) the firing rates during no-stop trials in three epochs: a) the period of
381 400 ms during the holding time preceding the appearance of the target; b) the RT epoch;
382 c) the movement time (MT) epoch, defined as the time window between movement onset
383 and the time when the target was touched. A cell was classified as reaching-related if it
384 showed a main effect at the ANOVA and if post hoc analysis (Tukey Kramer test; p<

0.05) revealed that the firing rate during the RT and/or the MT epoch differed from the discharge in the 400 ms epoch before target onset. The results of this analysis showed that 154 neurons (94.5 %) had a main effect ($p<0.05$), namely were modulated during the task. Of major relevance, post hoc tests revealed that 22 neurons (14.3 %) significantly changed their discharge exclusively during the RT epoch; 19 neurons (12.3 %) were significantly modulated exclusively during the MT epoch; finally 113 neurons (73.4 %) showed a significant change of the firing rate both during the RT and MT epochs. Overall 135 neurons (87.6 %) were modulated during motor preparation, i.e., during the RT epoch. These neurons were those selected for further analyses in this paper because they showed a modulation before the start of the movement and could be potentially involved in its generation. Thus, selected neurons are those whose discharge was modulated during the preparation of the arm movement and therefore they are the best candidate to show a modulation of their firing rate according to the fact that a movement should be executed or not.

Cancellation signals for reaching movements in PMd

To determine whether and how PMd neurons, with significant activity during the RT, were involved in inhibiting a planned arm movement, we compared the activity of the 135 neurons in those trials in which reaching movements were executed (no-stop trials) versus trials in which they were successfully inhibited (stop-success trials).

To influence the behaviour, a reaching-related cell must change its discharge when a reaching movement is executed with respect to when it is inhibited. Moreover to be causally involved in movement suppression, the divergence in neural activity should

408 take place before the behavioural estimate of the end of the cancellation process, i.e., the
409 SSRT (Hanes et al 1998; Parè and Hanes 2003). To this purpose, we analyzed data by
410 aligning neural activity to target presentation (go signal) and, since the stop signal
411 appears at different SSDs, we analysed the modulation of neural activity separately for
412 each SSD.

413 Figure 5 shows the activity, aligned to target presentation, for two example
414 neurons recorded during the same session (Monkey S; arm movements directed toward a
415 right target; SSD of about 300 ms). For both neurons, the activity during stop-success
416 trials is compared with the activity recorded during latency matched no-stop trials (see
417 Methods). The figure also reports the traces of the horizontal component of eye
418 movements during stop-success and latency matched no-stop trials. In no-stop trials, the
419 monkey always moves the eyes toward the target after its appearance; in addition during
420 stop trials, it moves back the gaze to the center of the screen as soon as the stop signal
421 appears. For both neurons, the activity of no-stop trials starts to increase about 150-200
422 ms after the go-signal and peaks at about 100 ms before the average time of movement
423 onset (Figure 5; M_on). During successful stop trials the activity of both neurons initially
424 resembles that of no stop trials. However, after the stop signal appearance, for one
425 neuron, thereafter named “type A” neuron, the activity significantly decreases after stop
426 signal presentation with respect to that recorded during latency matched no-stop trials
427 (Figure 5A) while for the other, hereafter named “type B” neuron, the activity
428 significantly increases (Figure 5B). The differential spike density functions (lower panels
429 of Figure 5) indicate that a significant divergence (see Methods) occurs before the end of
430 the SSRT for both the type A (neural cancellation time: -74 ms) and type B neuron

(neural cancellation time: -63 ms). This divergence is well before (about 200 ms) the average time of movement onset (M_on; Figure 5).

The estimate of the neural cancellation time of the 388 computable SSDs (namely, those SSDs presented at least 20 times in the recording block of trials and with at least 5 trials correctly executed) is presented in Figure 6A for the 263 with a significant differential activation (see Methods). In 153/263 (58.2%) SSDs the cancellation time preceded the end of SSRT by 48.6 (± 2.4 SE) ms on average. The number is still consistent (88/263; 33.5%) when considering only neural cancellation times shorter than the value obtained by subtracting from the SSRT, the estimated average delay (50 ms) needed for neural activity in PMd to influence arm muscle activity (Lemon et al. 1986; McKiernan et al. 1998; Morrow and Miller 2002; Tokuno and Nambu 2000).

In order to give an account of the countermanding modulation in terms of number of cells we used the following procedure. We assessed the number of neurons in which at least 60% of their SSDs[1] showed a significant countermanding-related modulation (i.e., a cancellation time < SSRT). We found that 44/135 (32.6%) neurons showed such a modulation. When considering the 50 ms efferent delay, the number of neurons with a countermanding behavior becomes 34/135 (25%), still a consistent population.

As stated above we found two different types of countermanding modulation: type A and type B. In order to evaluate the frequency of these two neural behaviours, for each SSD with a significant countermanding related modulation we computed a normalized index of the discharge rate (IDR; Figure 6B):

[1] We choose the 60% of SSDs as threshold to define a cell as a "countermanding neuron" because this is a very conservative estimate. In fact, when considering the fixed-SSD procedure, 60% means that at least 3 out of 4 SSDs have to show a significant countermanding-related modulation. On the other hand when considering the staircase procedure, since each recorded cell had generally 2 SSDs analyzable (see Methods), 60% means that all SSDs have to show a significant countermanding-related modulation.

452 $$IDR= (NoST-ST)/(NoST+ST)$$

453 where ST and NoST represent the activity during stop-success trials and latency matched
454 no-stop trials, respectively, in a 50 ms window centered on the end of the SSRT. The
455 index can take a negative value up to minus one, when the cell discharged only during
456 stop-success trials, corresponding to a neural modulation similar to that reported in
457 Figure 5B (type B), or a positive value, up to plus one corresponding to the absence of
458 activity during stop-success trials at the end of SSRT, corresponding to a neural
459 modulation similar to that reported in figure 5A (type A). As shown in Figure 6B, the
460 number of SSDs with positive IDRs was higher than the number of SSDs with negative
461 IDRs, 94 vs 59 respectively (χ^2 test, $p<0.005$). Of the 44 neurons exhibiting
462 countermanding related modulation, 26 had positive IDRs and 18 had negative IDRs.
463 Interestingly, a neuron exhibiting a countermanding modulation always showed the same
464 type of response for each SSD analysed. In addition, a one-way-ANOVA (four levels:
465 cancellation time at SSD1, SSD2, SSD3, SSD4) revealed that cancellation time did not
466 change as a function of SSDs length ($F [1,3]= 1.6$, $p=0.23$). We controlled for differences
467 in the neural cancellation time of the two classes of neurons. The activity started to
468 diverge on average 46 ± 3.3 ms and 52.6 ± 3.1 ms before the end of the SSRT in type A
469 and type B neurons respectively. Statistical analysis showed that in the two classes of
470 neurons the activity in stop-success trials diverges from that of latency matched no stop
471 trials at the same time (t-test, $df=151$, $t= 1.4$, $p =0.17$).

472 Since we had a restricted subset of neurons with a movement-preparatory activity
473 for which the behavioral control was good in both directions of movement (76/135 or
474 56%), we analyzed the neural activity of those cells to shed light on whether i) neurons

countermand a movement in both directions or just in one direction, and ii) countermanding behavior differs between neurons that have a preferred direction versus those that do not have it.

First of all, for each of these neurons, we considered those SSDs that were computable (see Methods) in both directions. Overall these SSDs were 181/388, of those 99 showed a countermanding related modulation. 45/99 SSDs showed a countermanding behavior in both direction of movements, while 54/99 did not. The frequency of the two types of SSD was not different (χ^2=0.37). Importantly, a neuron showing a countermanding modulation in one or in both movement directions did so at all its SSDs. Therefore we found two groups of neurons: one that countermanded in both movement directions and the other that countermanded jut in one.

In principle it could postulated that neurons having a directional tuning, might have a different modulation even for movement suppression. A visual inspection revealed that often the neuronal discharge during the during no-stop trials was higher in one direction than in the opposite one. We quantitatively assessed the number of cells exhibiting a preferred direction comparing with a t-test the firing rates of no-stop trials during the RT epoch. We found that the majority of cells were directionally tuned (59/76 or 77.6%). Among cells with a preferred direction 35/59 SSDs showed a countermanding behavior in both direction of movements, and 24/59 did not, their frequency was not significantly different (χ^2=0.26). The same was true for non-directionally tuned neurons (10/17 SSDs had a countermanding modulation in both movement direction and nine just in one; χ^2=0.82). Thus directional tuning does not seem to affect the countermanding behavior of PMd neurons. However we are aware that our task is not ideal for tackling

498 the relationship between directional tuning and countermanding modulation, given that
499 we did not test the neurons in more than two directions. Further studies need to be
500 performed to clarify this issue.

501 Finally, since we recorded from both the rostral and caudal portion of PMd, and it
502 is known that these two regions have different proportions of reaching related neurons
503 and signal/motor-related activities (Johnson et al 1996; Hoshi and Tanji 2006), we
504 explored i) whether either the distribution of type A and type B countermanding neurons
505 have a different distribution along the rostrocaudal dimension; ii) whether neurons with a
506 'motor' prevalent activity display a different modulation during the countermanding task
507 with respect to those with a 'visual' prevalent activity. We found that there were no
508 evident clusters or gradients of cells properties in the tangential cortical domain explored
509 (Figure 1A). As far as the second argument is concerned, for each neuron exhibiting a
510 significant countermanding modulation (44/135), following the logic of Ray et al (2009),
511 we computed a visual-movement index (VMI) as follows: VMI= (MA - VA)/(MA +
512 VA), where VA stands for visual activity and MA stands for movement activity. Since
513 the two animals had a different average RT (see table 1) the time windows for the
514 computation of the mean firing rates were different for the two monkeys. The time
515 window of VA was 50–200 ms and 50-170 after go-signal onset for monkey S and
516 monkey L, respectively. The time window of MA was -100 +50 ms and -70 +50 after
517 movement onset for monkey S and monkey L, respectively. Neurons with negative values
518 of VMI represent cells for which visually evoked response is prevalent (VP=visual
519 prevalent cells), while neurons with positive values of VMI represent cells for with
520 prevalent arm movement-related activity (MP=movement prevalent cells). First of all we

looked at whether VP and MP had a different distribution among the population of countermanding cells. 25/44 resulted MP-neurons (about 57%) while 19/44 were VP-neurons. The difference is not significative (χ^2-test, p=0.36). On average the VMI was 0.45±0.06 and -0.37±0.06 for MP- and VP-neurons respectively (t-test, t(42)=9.54, p<0.001). Secondly we compared the cancellation time of all MP- and VP-neurons measured at each computable SSD. On average the cancellation time preceded the SSRT of 46.1 ± 3.4 ms and of 51.5 ± 3.8 ms for the MP- and for the VP-neurons, respectively. There was not a significant difference (either using a parametric test, t-test, t(114)=1.02, p=0.31, or a non-parametric test, Kolmogorov-Smirnov test, p=0.11). In conclusion, both neuronal types play a similar role as far as the production and the suppression of an arm reaching movement is concerned, in contrast to what found by Ray et al (2009) in FEF, further suggesting that oculomotor centers have a different functional organization with respect to brain areas controlling arm movements.

Interpretational issues about the countermanding modulation of PMd neurons

We have interpreted the modulations of PMd neurons as they were related to the production or the cancellation of pending reaching arm movements. However, at least in principle it is possible that PMd neuronal activity could be related to other processes. In fact PMd activity may have been linked to eye movements/gaze position (Boussaoud et al 1993; Boussaoud et al 1998; Fujii et al 2000; Pesaran et al 2006; Pesaran et al 2010) or to the visual presentation of the stop-signal.

First of all we assessed the relationship between saccadic and arm movements during the task. As expected (Carey 2000), the eyes on average reacted to the target

presentation faster than the arm (Kolmogorov-Smirnov test, p*s*<0.001). However, the saccadic RT of monkey L was longer than that of monkey S (325.7 ± 5.8 and 194.9 ± 7 ms, respectively, Kolmogorov-Smirnov test, p*s*<0.001). As a consequence, the difference between the RTs of arm and eye was bigger for monkeys S (mean difference 303.2 ± 7.3 ms) than for monkey L (mean difference 35.8 ± 3.3 ms, t-test df = 43, t=-34.3, p<0.0001). Two animals employed different ocular strategies during the countermanding task. In no stop trials, monkey S quickly moved the eyes towards the peripheral target while the arm movements were procrastinated (Figure 5), conversely monkey L made saccades to the target just before executing the arm movements (Figure 7). Probably these differences account for the very different ocular behaviour displayed during stop trials by the two animals. During stop-success trials, monkey L did not move the gaze from the central position in stop-success trials (Figure 7; lower panels). Conversely, monkey S first made a saccade toward the peripheral target, as for no stop trials, and after the presentation of the stop signal, it moved back the eyes on it (Figure 5). Nevertheless, in spite of the very different patterns of eye movements displayed by the two monkeys during SSRT, the neural modulation during the countermanding task was very similar, as shown for the example neurons of Figure 5 and 7. In both monkeys, type A/B neurons decreased/increased their discharge during stop-success trials after the stop signal presentation and before the end of the SSRT.

The oculomotor strategy of Monkey S allows us to further tackle the issue of the possible relation between the neural modulation and eye movements. The peak of activity shown during successful stop trials of the neuron shown in fig 5B might seem to be related to the eye movement following stop signal appearance (or to a visual related

567 activation). We excluded the possibility for this neuron, and for all of the other neurons
568 showing both movement-preparatory activity and countermanding modulation in Monkey
569 S, by comparing the neural activity elicited by eye movements with similar vectors
570 occurring during different phases of the task. Figure 8 shows, for the same neuron shown
571 in Figure 5B the activity during stop-success trials compared with the activity obtained in
572 the stop-failure trials for the two positions in which the target could appear. During stop-
573 success trials, the monkey exhibits a pattern of eye movements qualitatively similar for
574 both target positions. When the target appears to the left (fig 8A), the monkey performs
575 first a leftward eye movement and, after appearance of the stop signal, it makes a
576 rightward saccade. Exactly the opposite eye movement sequence takes place when the
577 target is presented to the right. Thus the peak of neural activity observed during the SSRT
578 cannot be related either: i) to the immediately following eye movement because a similar
579 saccade does not elicit a similar neural modulation (e.g. compare the activity during stop-
580 success trials after rightward eye movements in panel 8A and 8B); or ii) to a visual
581 response since it does not appear in stop-failure trials even though the stop signal was
582 presented exactly at the same time as in success-stop trials. All type B neurons, with a
583 pattern of activity similar to that shown by the neuron of Figure 5B, were analyzed in this
584 way and in all cases we have been able to exclude that their neural modulation could be
585 linked either to eye movement generation and/or sensory stimulation

586 On the ground of our experimental evidence we strongly believe that our results
587 cannot be explained on the basis of gaze-related and/or saccade-related modulations.
588 Instead our findings indicate the presence of a subpopulation of PMd reaching related

589 neurons that displays a modulation of activity which is potentially able to control the
590 production and the suppression of arm movements.
591
592

DISCUSSION

Neural signals for reaching movements inhibition in PMd

The main goal of the present study was to explore the contribution of single neurons of PMd cortex in inhibiting a planned reaching arm movement. Thus, among recorded neurons, we selected those modulated during the preparation of the movement and we found that a substantial percentage of these neurons exhibit, after stop signal presentation, a pattern of activity able to influence the production or the cancellation of reaching arm movements.

Historically, single unit studies have shown that PMd is involved in several aspects of arm movement control. PMd neurons, also thanks to the direct access to the spinal cord (Dum and Strick, 1996), have a role in the preparation of movements (Churchland et al 2006; Crammond and Kalaska 2000; Johnson et al 1996; Weinrich and Wise 1982), in learning associations between sensory stimuli and motor responses (Di Pellegrino and Wise 1993; Wise et al 1983), in online correction of arm movements (Georgopoulos et al 1983), in the representation of potential actions (Cisek and Kalaska 2005). To our knowledge, there is just one study showing that neural activity of PMd neurons changes when a movement is suppressed with respect to when it is executed in a Go/No-Go paradigm (Kalaska and Crammond 1995). However in the Go/No-Go task the signal for inhibiting the movement is presented before the go signal, while in the countermanding the stop follows the go signal. Hence in the Go/No-Go task it is a potential movement and not an ongoing response that has to be cancelled.

In our sample more than one third of neurons involved in movement preparation exhibited a countermanding modulation. In these cells the discharge changed when a

616 reaching movement was executed with respect to when it was inhibited and this change
617 preceded the end of the behavioral estimate of movement cancellation (the SSRT). We
618 identified two types of cells showing this neuronal pattern. In the most common class of
619 neurons, type A, the activity during stop-success trials decreases before the end of the
620 SSRT with respect to that recorded during no-stop trials. In type B neurons, movement
621 suppression is associated with a temporary increase of activity with respect to the activity
622 recorded during no-stop trials.

623 The behaviour of the two classes of neurons we observed resembles, at a first
624 glance, that of movement and fixation neurons in the FEF (Hanes et al 1998) and in the
625 SC (Paré and Hanes 2003). However while the parallel between type A and movement
626 neurons might be supported the one for type B and fixation neurons cannot. In fact
627 fixation neurons are tonically active during fixation periods while they drastically reduce
628 their activity just before the execution of a saccade (Munoz and Wurtz 1993). During
629 stop-success trials, fixation neurons in FEF and SC increase their discharge after stop
630 signal presentation (Hanes et al 1998; Paré and Hanes 2003). This increment counteracts
631 the decrease of the discharge occurring after the presentation of the go signal, allowing
632 fixation cells to reestablish the level of activity typical of fixation periods, in agreement
633 with a system based on a finely controlled gating mechanism (Munoz and Wurtz 1993).
634 Differently, type B neurons do not display a tonic discharge when the arm is maintained
635 still and after stop signal presentation they increase their activity faster than in those trials
636 where a movement has to be produced. In addition fixation neurons have an important
637 role during saccade generation since they control the discharge of omnipause neurons
638 (OPNs) in the nucleus raphe interpositus. In fact to generate a saccade the tonic inhibition

639 of OPNs on the 'burst neurons' in the brain stem needs to be removed (Bergeron and
640 Guitton 2002; Munoz and Wurtz 1993).

641 However it is important to remark, as further suggested by our findings, that the
642 functional organization for saccades control in the oculomotor centers does not have a
643 correspondent in the neural structures controlling arm movements. The overall
644 organization of arm movement control is much more complicated. In principle it would
645 be possible to speculate that inhibitory interneurons of PMd-M1 could prevent movement
646 execution during the planning of an action by suppressing the activity of corticospinal
647 movement neurons. In this frame the action would start when cortical inhibition would be
648 removed. However, recent evidences (Kaufman et al 2010; Merchant et al 2008) show
649 that inhibitory interneurons in PMd and M1 increase and not decrease their discharge at
650 the time of movement generation. Therefore, these neurons do not seem to participate to
651 movement control as fixation neurons. In addition interneurons in PMd are more active
652 during both the preparatory phases of a reaching movement and around movement onset,
653 than putative pyramidal neurons (Kaufman et al 2010). PMd is able not only to influence
654 the neural activity of interneurons in the spinal cord (Dum and Strick 2002; Prut and Fetz
655 1999) but also to excite or inhibit M1 (Ghosh and Porter 1988; Tokuno and Nambu
656 2000). Overall, these results strongly suggest that the control of arm movements is
657 organized very differently with respect to that of eye movements. Possibly type A
658 neurons could correspond to PMd projection neurons, directed, e.g., to M1 or to spinal
659 cord interneurons (Dum and Strick 2002), while type B neurons could correspond to PMd
660 inhibitory interneurons, actively controlling the discharge of type A neurons.
661 Unfortunately we have no further argument to support this idea since we could no

662 classify neurons on the basis of the recorded waveforms (Kaufman et al 2010; Mitchell et
663 al 2007). This topic will be object of future researches together with the description of the
664 neural modulation in M1 during a countermanding task.

665 Another possibility, to explain the different behaviour of type A and type B
666 neurons in the countermanding task, is that the decrease of discharge of the type A
667 neurons would correspond to the suppression of agonist muscles of the arm for a given
668 movement, while the increase of type B would correspond to the activation of the
669 antagonist muscles. This way the activity eventually elicited in the agonist muscles, after
670 the presentation of the go signal would be suppressed and contrasted at the same time.
671 Results by Kudo and Ohtsuki (1998) provide support to this hypothesis, especially for
672 long SSDs when the agonist muscles are more likely to be activated. In contrast, a recent
673 report did not find evidence for co-contraction of antagonist muscles during movement
674 suppression in a countermanding task (Scangos and Stuphorn 2010). Scangos and
675 Stuphorn (2010) suggest that action inhibition is accomplished by relaxing the agonist
676 muscle. The discrepancy could be explained by the different arm movements required in
677 the two experiments: in one case subjects were asked to control the elbow movements by
678 (Kudo and Ohtsuki 1998) in the other the monkeys have to move an handlebar (Scangos
679 and Stuphorn 2010). However, Toma et al (1999), using the functional magnetic
680 resonance, showed that not only muscle contraction but also muscle relaxation produces a
681 transient increase of activity in the M1 contralateral to the limb used and bilaterally both
682 in the supplementary motor areas and PMd. Thus the peak of activity observed in type B
683 neurons could be associated with the active relaxation of agonist muscles. In line with
684 this hypothesis, it has been shown that suppression of the muscle contraction can occur as

685 a consequence of the discharge of M1 projection neurons likely targeting spinal
686 inhibitory interneurons (Cheney et al. 1985; Lemon et al. 1987). Unfortunately, we
687 cannot further argument on this issue because for technical reasons we have been unable
688 to use data obtained during electromyography of selected muscles. Further studies are
689 needed to clarify this point. However it is important to underline that the lack of EMG
690 recordings should not impact too much our findings. In fact, if we assume that our
691 monkeys used the arm muscles as the monkeys recorded by Scangos and Stuphorn
692 (2010), we could exploit their observations to interpret the relationship between muscle
693 activity and neural modulation. The average cancellation time for muscles reported by
694 Scangos and Stuphorn (2010) preceded of 25 ms the SSRT. In our sample the average
695 cancellation time for PMd neurons was about 50 before the SSRT, therefore in time to
696 drive muscle activity. In addition, we found that neuronal activity of countermanding
697 cells is likely to be dissociated from muscle activity, as the difference between the
698 estimated SSRT and the neural cancellation time does not increase as a function of the
699 SSDs' length.
700
701 **The role of PMd in the brain inhibitory network**
702 In humans, it has been suggested that the ability of withholding manual motor responses
703 relies critically on the action of a right lateralized fronto-basal-ganglia-thalamic pathway
704 in the motor regions. This network comprises two areas of the frontal cortex, the IFC
705 (Aron et al 2003; Aron et al 2007; Chambers et al 2006) and pre-SMA (Aron et al 2007;
706 Floden and Stuss 2006; Nachev et al 2007). Both areas are thought to modulate the
707 cortical neural processes for movement initiation via the hyperdirect route, passing

through the subthalamic nucleus (Aron and Poldrack 2006; Aron et al 2007; van den Wildenberg et al 2006). Recently, Li et al (2008) demonstrated that the head of the caudate nucleus plays a key function in movement suppression.

In monkeys, during an arm countermanding task, Scangos and Stuphorn (2010) found that the activity of SMA and pre-SMA neurons is not sufficient to control arm movement initiation because the great majority of cells with movement–related activity did not change their activity when a reach was performed with respect to when it was cancelled. However, since the discharge of movement–related neurons was reward contingent, Scangos and Stuphorn (2010) concluded that the activity in SMA and pre-SMA represents the motivation for performing a given action, that is the "urge to act".

Scangos and Stuphorn (2010) found also a small percentage of neurons (~2%) that exhibit a countermanding modulation. Those neurons very likely participate to arm movement suppression. The involvement of SMA inhibition of unwanted movements in reaction to the presentation of a stop signal, has been confirmed by Chen et al (2010), who showed changes of LPFs power at low frequencies (10-50 Hz) occurring early enough to be causally involved in movement cancellation. In addition Chen et al (2010) demonstrated that SMA plays a key role in proactive control, a form of anticipatory control which, on the basis of known task demands (e.g. presence/absence of stop signal, frequency of stop signals), leads to systematic adjustments of the behavioral performance aimed to enhance the chance of correctly suppress a movement. However the low percentage of countermanding neurons found in SMA and pre-SMA areas question the extent to which those regions are truly involved in the process of suppressing a movement after the appearance of a stop signal. The LFP modulation observed in SMA

731 by Chen et al (2010), might in fact not be due to the activity of local neurons but to inputs
732 coming from other brain regions (Logothetis, 2003; Mattia et al 2010) which might
733 provide a source for proactive control.

734 Even though the exact role of each of these brain regions remains controversial,
735 there is no doubt that their actions have to be exerted through the motor areas. M1
736 neurons with preparatory activity are a target of SMA output neurons with preparatory
737 activity (Aizawa and Tanji, 1994; Tanji and Kurata, 1985). Somehow neural signals of
738 the motor cortex have to be shaped so that the descending commands to the spinal cord
739 (or to the brainstem) can halt a planned movement. Using the transcranial magnetic
740 stimulation, Coxon et al. (2006) demonstrated the involvement of M1 in inhibitory
741 processes. Furthermore, Picton et al. (2007) in humans, and Moll and Kuypers (1977) in
742 monkeys pointed out the role of PMd in inhibition, showing that reaching movements
743 become more impulsive and uncontrolled after selective damage to this area.

744 These studies however could not uncover the neural mechanisms underlining the
745 suppression processes. Our study shows, for the first time, the existence of two types of
746 neurons in PMd whose activity significantly change before reaching arm movement are
747 successfully countermanded in response to a visual stop signal. Thus, we have found that
748 in PMd, a substantial proportion of cells produces signals able to participate to the
749 distributed process controlling the execution or the suppression of an arm movement.
750

BIBLIOGRAPHY

Aizawa H, Tanji J. Corticocortical and thalamocortical responses of neurons in the monkey primary motor cortex and their relation to a trained motor task. *J Neurophysiol* 71: 550-60, 1994.

Aron AR, Behrens TE, Smith S, Frank MJ, Poldrack RA. Triangulating a cognitive control network using diffusion-weighted magnetic resonance imaging (MRI) and functional MRI. *J Neurosci* 27:3743-3752, 2007.

Aron AR, Fletcher PC, Bullmore ET, Sahakian BJ, Robbins TW. Stop-signal inhibition disrupted by damage to right inferior frontal gyrus in humans. *Nat Neurosci* 6: 115-116, 2003.

Aron AR, Poldrack RA. Cortical and subcortical contributions to Stop signal response inhibition: role of the subthalamic nucleus. *J Neurosci* 26: 2424-2433, 2006.

Band GP, van der Molen MW, Logan GD. Horse-race model simulations of the stop-signal procedure. *Acta Psychol (Amst*) 112:105-142, 2003.

Bergeron A, Guitton D. In multiple-step gaze shifts: omnipause (OPNs) and collicular fixation neurons encode gaze position error; OPNs gate saccades. *J Neurophysiol* 88: 1726-1742, 2002

Boucher L, Palmeri TJ, Logan GD, Schall JD. Inhibitory control in mind and brain: an interactive race model of countermanding saccades. *Psychol Rev* 114: 376-397, 2007.

Biittner-Ennever JA, Cohen B, Pause M, Fries W. Raphe nucleus of the pons containing omrdpause neurons of the oculomotor system in the monkey, and its homologue in man. *J Comp Neurol* 267:307-321, 1988.

Carey DP. Eye-hand coordination: eye to hand or hand to eye? *Current Biology* 10: R416-R419, 2000.

Chambers CD, Bellgrove MA, Stokes MG, Henderson TR, Garavan H, Robertson IH, Morris AP, Mattingley JB. Executive "brake failure" following deactivation of human frontal lobe. *J Cogn Neurosci* 18: 444-455, 2006.

Chen X, Scangos KW, Stuphorn V. Supplementary motor area exerts proactive and reactive control of arm movements. *J Neurosci*. 30:14657-75, 2010.

Cheney PD, Fetz EE. Functional classes of primate corticomotoneuronal cells and their relation to active force. *J Neurophysiol* 44:773-791, 1980.

Cheney PD, Fetz EE, Palmer SS. Patterns of facilitation and suppression of antagonist forelimb muscles from motor cortex sites in the awake monkey. *J Neurophysiol* 53:805-820, 1985.

Churchland MM, Shenoy KV. Delay of movement caused by disruption of cortical preparatory activity. *J Neurophysiol* 97: 348-359, 2007.

Churchland MM, Yu BM, Ryu SI, Santhanam G, Shenoy KV. Neural variability in premotor cortex provides a signature of motor preparation. *J Neurosci* 26: 3697-3712, 2006.

Cisek P, Kalaska JF. Neural correlates of reaching decisions in dorsal premotor cortex: specification of multiple direction choices and final selection of action. *Neuron* 45:801-814, 2005.

Coxon JP, Stinear CM, Byblow WD. Intracortical inhibition during volitional inhibition of prepared action. *J Neurophysiol* 95: 3371-3383, 2006.

795 **Crammond DJ, Kalaska JF**. Prior information in motor and premotor cortex: activity
796 during the delay period and effect on pre-movement activity. *J Neurophysiol* 84: 986-
797 1005, 2000.
798 **Di Pellegrino G, Wise SP**. Effects of attention on visuomotor activity in the premotor
799 and prefrontal cortex of a primate. *Somatosens Mot Res* 10: 245-262, 1993.
800 **Dum RP, Strick PL.** Spinal cord terminations of the medial wall motor areas in macaque
801 monkeys. *J Neurosci* 16:6513-6525, 1996.
802 **Dum RP, Strick, PL**. Motor areas in the frontal lobe of the primate. *Physiol Behav* 77:
803 677–682, 2002.
804 **Evarts EV.** Relation of pyramidal tract activity to force exerted during voluntary
805 movement. *J Neurophysiol* 31:14-27, 1968.
806 **Floden D, Stuss DT.** Inhibitory control is slowed in patients with right superior medial
807 frontal damage. *J Cogn Neurosci* 18:1843-1849, 2006.
808 **Fuchs AF, Robinson DA.** A method for measuring horizontal and vertical eye
809 movement chronically in the monkey. *J Appl Physiol* 21:1068-1070, 1966.
810 **Georgopoulos AP, Kalaska JF, Caminiti R, Massey JT**. Interruption of motor cortical
811 discharge subserving aimed arm movements. *Exp Brain Res* 49: 327-340, 1983.
812 **Ghosh S, Porter R.** Corticocortical synaptic influences on morphologically identified
813 pyramidal neurons in the motor cortex of the monkey. *J Physiol* 400: 617–629, 1988.
814 **Hanes DP, Patterson WF, Schall JD.** Role of frontal eye fields in countermanding
815 saccades: visual, movement, and fixation activity. *J Neurophysiol* 79: 817-834, 1998.
816 **Hanes DP, Schall JD**. Countermanding saccades in macaque.*Vis Neurosci* 12:929-37,
817 1995.

Hoshi E, Tanji J. Differential involvement of neurons in the dorsal and ventral premotor cortex during processing of visual signals for action planning. *J Neurophysiol* 95: 3596-616, 2006.

Logothetis NK The underpinnings of the BOLD functional magnetic resonance imaging signal. *J Neurosci.* 23:3963-71, 2003

Ito S, Stuphorn V, Brown JW, Schall JD. Performance monitoring by the anterior cingulate cortex during saccade countermanding. *Science* 302:120-122, 2003.

Johnson PB, Ferraina S, Bianchi L, Caminiti R. Cortical networks for visual reaching: physiological and anatomical organization of frontal and parietal lobe arm regions. *Cereb Cortex* 6:102-119, 1996.

Kalaska JF, Crammond DJ. Deciding not to GO: neuronal correlates of response selection in a GO/NOGO task in primate premotor and parietal cortex. *Cereb Cortex* 5: 410-428, 1995.

Kaufman MT, Churchland MM, Santhanam G, Yu BM, Afshar A, Ryu SI, Shenoy KV. Roles of monkey premotor neuron classes in movement preparation and execution. *J Neurophysiol* 104: 799-810, 2010.

Kudo K, Ohtsuki T. Functional modification of agonist-antagonist electromyographic activity for rapid movement inhibition. *Exp* Brain Res 122:23-30, 1998.

Lemon RN, Mantel GW, Muir RB. Corticospinal facilitation of hand muscles during voluntary movement in the conscious monkey. *J Physiol* 381:497–527, 1986.

Lemon RN, Muir RB, Mantel GW. The effects upon the activity of hand and forearm muscles of intracortical stimulation in the vicinity of corticomotor neurones in the conscious monkey. *Exp Brain Res* 66:621-637, 1987.

841 **Levitt H**. Transformed up-down method in psychoacustics. *J Acoust Soc Am* 49: 467–
842 477, 1971.
843 **Li CS, Yan P, Sinha R, Lee TW**. Subcortical processes of motor response inhibition
844 during a stop signal task. *Neuroimage* 41:1352-1363, 2008.
845 **Logan GD.** On the ability to inhibit thought and action: A users' guide to the stop signal
846 paradigm. In: *Inhibitory Processes in Attention, Memory and Language*, edited by
847 Dagenbach D, Carr TH: San Diego: Academic Press, 1994, p. 189-239.
848 **Logan GD, Cowan WB**. On the ability to inhibit thought and action: A theory of an act
849 of control. *Psychol Rev* 91:295-327, 1984.
850 **Mattia M, Ferraina S, Del Giudice P.** Dissociated multi-unit activity and local field
851 potentials: A theory inspired analysis of a motor decision task. *Neuroimage* 52:812-823,
852 2010.
853 **McKiernan BJ, Marcario JK, Karrer JH, Cheney PD.** Corticomotoneuronal postspike
854 effects in shoulder, elbow, wrist, digit and intrinsic hand muscles during a reach and
855 prehension task. *J Neurophysiol* 80: 1961-1980, 1998.
856 **Merchant H, Naselaris T, Georgopoulos AP.** Dynamic sculpting of directional tuning
857 in the primate motor cortex during three-dimensional reaching. *J Neurosci* 28: 9164–
858 9172, 2008.
859 **Miller J, Riehle A, Requin J**. Effects of preliminary perceptual output on neuronal
860 activity of the primary motor cortex. *J Exp Psychol Hum Percept Perform* 18:1121-1138,
861 1992.
862 **Mirabella G, Pani P, Paré M, Ferraina S.** Inhibitory control of reaching movements in
863 humans. *Exp Brain Res* 174: 240-255, 2006.

Mirabella G, Pani P, Ferraina S. Context influences on the preparation and execution of reaching movements. *Cogn Neuropsychol* 25: 996-1010, 2008.

Mirabella G, Pani P, Ferraina S. The presence of visual gap affects the duration of stopping process. *Exp Brain Res* 192:199-209, 2009.

Mitchell JF, Sundberg KA, Reynolds JH. Differential attention-dependent response modulation across cell classes in macaque visual area v4. *Neuron* 55: 131-141, 2007.

Moll L, Kuypers HG. Premotor cortical ablations in monkeys: contralateral changes in visually guided reaching behavior. *Science* 198:317-319, 1977.

Morrow MM, Miller LE. Prediction of muscle activity by populations of sequentially recorded primary motor cortex neurons. *J Neurophysiol* 89: 2279-2288, 2003.

Munoz DP, Wurtz RH. Fixation cells in monkey superior colliculus. I. Characteristics of cell discharge. *J Neurophysiol* 70:559-575, 1993.

Nachev P, Wydell H, O'neill K, Husain M, Kennard C. The role of the pre-supplementary motor area in the control of action. *Neuroimage* 36: Suppl 2:T155-T163, 2007.

Osman A, Kornblum S, Meyer DE. The point of no return in choice reaction time: controlled and ballistic stages of response preparation. *J Exp Psychol Hum Percept Perform* 12, 243-258, 1986.

Osman A, Kornblum S, Meyer DE. Does motor programming necessitate response execution? *J Exp Psychol Hum Percept Perform* 16:183-198, 1990.

Paré M, Hanes DP. Controlled movement processing: superior colliculus activity associated with countermanded saccades. *J Neurosci* 23: 6480-6489, 2003.

886 **Paxinos G, Huang XF, Toga AW.** *The Rhesus Monkey Brain in Stereotaxic*
887 *Coordinates*. San Diego: Academic Press, 2000.
888 **Picton TW, Stuss DT, Alexander MP, Shallice T, Binns MA, Gillingham S.** Effects of
889 focal frontal lesions on response inhibition. *Cereb Cortex* 17:826-838, 2007.
890 **Port NL, Kruse W, Lee D, Georgopoulos AP.** Motor cortical activity during
891 interception of moving targets. *J Cogn Neurosci* 13:306-318, 2001.
892 **Prut Y, Fetz EE** Primate spinal interneurons show pre-movement instructed delay
893 activity. *Nature* 401:590–594, 1999.
894 **Ray S, Pouget P, Schall JD.** Functional Distinction Between Visuomovement and
895 Movement Neurons in Macaque Frontal Eye Field During Saccade Countermanding *J*
896 *Neurophysiol* 102:3091-100, 2009.
897 **Riehle A, Requin J**. The predictive value for performance speed of preparatory changes
898 in neuronal activity of the monkey motor and premotor cortex. *Behav Brain Res* 53: 35-
899 49, 1993**.**
900 **Robinson DA.** A Method of measuring eye movement using a scleral search coil in a
901 magnetic field. *IEEE Trans Biomed Eng* 10: 137-145, 1963.
902 **Rubia K, Smith AB, Brammer MJ, Taylor E.** Right inferior prefrontal cortex mediates
903 response inhibition while mesial prefrontal cortex is responsible for error detection.
904 *Neuroimage* 20:351-358, 2003.
905 **Scangos KW, Stuphorn V.** Medial frontal cortex motivates but does not control
906 movement initiation in the countermanding task. *J Neurosci* 30:1968-82, 2010.
907 **Stuphorn V, Taylor TL, Schall JD.** Performance monitoring by the supplementary eye
908 field. *Nature* 408:857-860, 2000.

Swann N, Tandon N, Canolty R, Ellmore TM, McEvoy LK, Dreyer S, DiSano M, Aron AR. Intracranial EEG reveals a time- and frequency-specific role for the right inferior frontal gyrus and primary motor cortex in stopping initiated responses. *J Neurosci* 29:12675-12685, 2009.

Tanji J, Kurata K. Contrasting neuronal activity in supplementary and precentral motor cortex of monkeys. I. Responses to instructions determining motor responses to forthcoming signals of different modalities. *J Neurophysiol* 53: 129-41, 1985.

Thach WT. Timing of activity in cerebellar dentate nucleus and cerebral motor cortex during prompt volitional movement. *Brain Res* 88:233-241, 1975.

Toma K, Honda M, Hanakawa T, Okada T, Fukuyama H, Ikeda A, Nishizawa S, Konishi, J, Shibasaki H. Activities of the primary and supplementary motor areas increase in preparation and execution of voluntary muscle relaxation: an event-related fMRI study. *J Neurosci* 19: 3527-3534, 1999.

Tokuno H, Nambu A. Organization of nonprimary motor cortical inputs on pyramidal and nonpyramidal tract neurons of primary motor cortex: An electrophysiological study in the macaque monkey. *Cereb Cortex* 10: 58–68, 2000.

van den Wildenberg WP, van Boxtel GJ, van der Molen MW, Bosch DA, Speelman JD, Brunia CH. Stimulation of the subthalamic region facilitates the selection and inhibition of motor responses in Parkinson's disease. *J Cogn Neurosci* 18: 626-636, 2006.

Weinrich M, Wise SP. The premotor cortex of the monkey. *J Neurosci* 2:1329-45, 1982.

Weinrich M, Wise SP, Mauritz KH. A neurophysiological study of the premotor cortex in the rhesus monkey. *Brain* 107: 385-414, 1984.

Wetherill GB *Sequential methods in statistic*. Methuen (eds) London, 1966.

932 **Wise SP, Weinrich M, Mauritz KH.** Motor aspects of cue-related neuronal activity in
933 premotor cortex of the rhesus monkey. *Brain Res* 260:301-305, 1993.
934
935

936 **FIGURE CAPTIONS**

937 Figure 1. **Recording sites and Countermanding task.** (A) Location of recording sites in
938 the two monkeys. The relative positions of the recording chambers (big circles) are
939 indicated over a standard model of rhesus monkey brain. Dots indicate the entry points of
940 electrodes. The recording locations of type A and type B neurons are also indicated.
941 Inside each chamber the position of the sulci is reported. AS arcuate sulcus, CS central
942 sulcus, PS principal sulcus. A color code is used to identify data from two monkeys
943 (black: monkey L; grey: monkey S). (B) Temporal sequence of the visual displays for no-
944 stop and stop trials in the countermanding reaching task. All trials began with the
945 presentation of a central stimulus. After a variable holding (500-800 ms), it disappeared
946 and simultaneously a target appeared acting as a go-signal. In the no-stop trials monkeys
947 had to execute a speeded reaching movement toward the peripheral target. On a fraction
948 of interleaved trials (33%) the central stimulus reappeared after variable delays (stop
949 signal delays, SSDs), instructing the monkey to inhibit movement initiation. In stop trials,
950 if monkey countermanded the planned movement keeping the arm on the central stimulus
951 the trials was scored as a stop-success trial. Otherwise the trial was scored as a stop-
952 failure trial.

953

954 Figure 2. **Logic underlying the race model. (A)** The race model represents the
955 performance in the countermanding task assuming that a go process (black line)
956 independently race against a stop process (grey line) toward a threshold (broken
957 horizontal line). The go and stop processes are triggered by the presentation of the target
958 and of the stop signal, respectively. In stop trials, if the stop process finishes before the
959 go process, the reaching movement is cancelled (A, top) and vice versa (A, bottom). **(B)**

960 Predictions of the outcome of the race between stop and go process for the longest SSD
961 of the fixed SSD procedure (see methods). Considering an hypothetical distribution of
962 no-stop trials' reaction times (RTs), the responses that escape inhibition should be those
963 corresponding to reaching movements that had RTs less than the sum between the SSD
964 and the SSRT. Therefore, in the example illustrated, subjects should inhibit the
965 movement just 15% of the times (dark region).
966
967 Figure 3. **Independence of go and stop processes in the countermanding task at**
968 **behavioral level**. **(A)** Cumulative distributions of RTs of no-stop trials versus that of
969 stop-failures trials in one example session of monkey L. As predicted by the race model,
970 the cumulative distribution of the RTs of stop-failure trials is significantly shifted to the
971 left respect to that of the no stop trials (Kolmogorov-Smirnov test; $p<0.0005$). **(B)**
972 Observed versus predicted RTs of stop-failure trials in the same session illustrated in
973 panel A. Vertical bars at each data point indicate one standard error of the mean. The
974 numbers above the data points indicate the number of stop-failure trials at each SSD.
975
976 Figure 4. **Behavioral control. (A)** Inhibition function (IF), represented by the best fit of
977 the Weibull function, (see methods for further details), for one representative recording
978 session of monkey L. **(B)** Average IF across all recording sessions with fixed-SSD
979 procedure for monkey L (black line) and monkey S (grey line). Data from individual
980 subjects were combined by averaging, for each single SSD, the probability of generating
981 a movement even though a stop signal was presented.
982

Figure 5. **Changes of activity driven by the stop signal onset in neurons modulated during the preparation of the movement.** The activity of two neurons, recorded from two different electrodes in the same session (Monkey S), is shown for no-stop and latency matched stop-success trials. In each panel the upper graph represents the raster plots of neural activity in no-stop trials. Below the horizontal components of eye movements during no-stop trials are represented. The raster plot in the third row represents the neural activity in stop successful trials. Just below the eye movements for stop success trials are displayed. The two lower graphs represent the spikes density functions for no-stop trials (black lines), for stop-success trials (grey lines) and the differential spike density functions (grey areas) respectively. The grey band represents the estimated duration of the SSRT in the session. **(A)** Neuron type A. **(B)** Neuron type B. M_on: average time of movement onset. SSRT: stop signal reaction time. Neural activity, and other plots, are aligned to target onset (vertical line).

Figure 6. **Modulation of neural activity during the countermanding reaching task across the population of cells modulated during the preparation of the movement**. **(A)** Distribution of neural cancellation time (i.e. the time at which the activity during stop-success and latency-matched no stop trials became different) with respect to the SSRT, across the population of SSDs with a significant divergence, of cells modulated during the preparation of the movement. Each SSD contributed for one data point. Negative values indicate those SSDs with a countermanding modulation (i.e., those where cancellation times take place before the end of SSRT) while positive values indicate those SSDs with a divergence occurring after the end of SSRT. **(B)** Distribution

1006 of the indexes of discharge rate (IDR, see Results for further details) for the SSDs with a
1007 cancellation time shorter than SSRT. Each SSD from each cell contributed with one data
1008 point. Positive values indicate SSDs where the activity during no stop trials exceeded that
1009 of stop-success trials (type A) and viceversa for negative values (type B).
1010
1011 Figure 7. **Eye movements and their relationship with countermanding related**
1012 **modulation in Monkey L**. Each panel shows the average spike density functions of no
1013 stop latency matched trials (black lines) and stop-success trials (grey lines) for one SSDs
1014 of "type A" countermanding neurons (left panels) and for one SSDs of "type B"
1015 countermanding neurons (right panels) recorded in the same session, for monkey L. The
1016 dashed black line represents the differential spike density function. The lower part of
1017 each panel shows the horizontal components of eye movements during no stop latency
1018 matched trials (upper part) and stop-success trials (lower part). Neural activity and eye
1019 movements are aligned on the go signal onset. The grey band represents the duration of
1020 the SSRT in the given session. M_on indicates the average time of movement onset. The
1021 dotted black line represents the threshold value for significant divergence, and C
1022 represents the cancellation time (see methods for further details).
1023
1024 Figure 8. **The activity of type B neurons is not related to saccade generation or to**
1025 **visual stimulation**. Comparison, for the neuron shown in Figure 5B, of neural activity
1026 during stop-success trials with activity during stop-failure trials. Panel **(A)** and panel **(B)**
1027 show, respectively, the discharge of the neuron when the stop signal was presented
1028 during the preparation of an arm movement toward the left and the right side. The

1029 sequences at the top show the eye (+) movements during the different phases of the task
1030 with respect to target and stop signal appearance. The horizontal component of the eye
1031 movements for stop-success and stop-failure trials are displayed in the lower panels. Plots
1032 are aligned to target onset (vertical line). The time of stop signal presentation is indicated
1033 (Stop). M_on indicates the average time of movement onset for stop-failure trials.

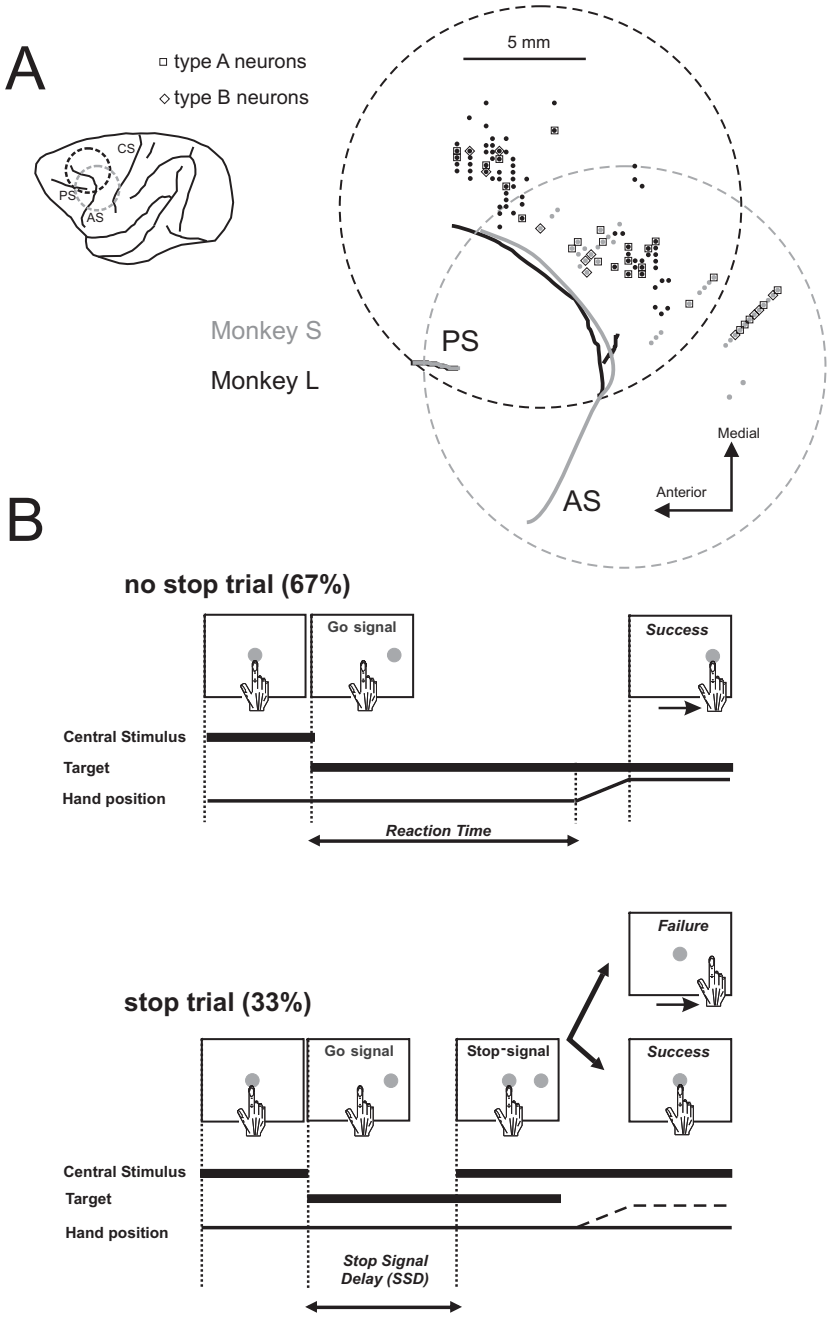

MIRABELLA ET AL., FIGURE 1

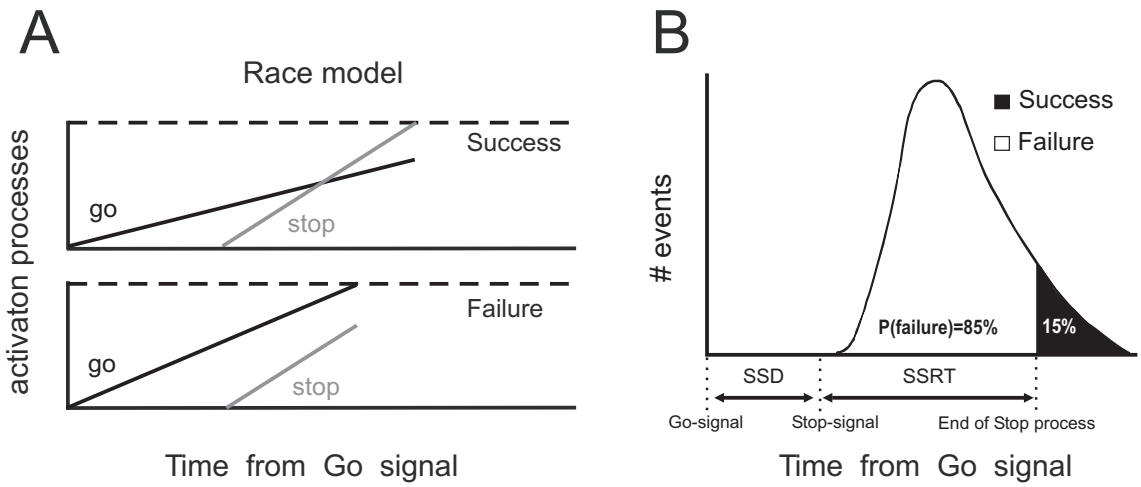

MIRABELLA ET AL., FIGURE 2

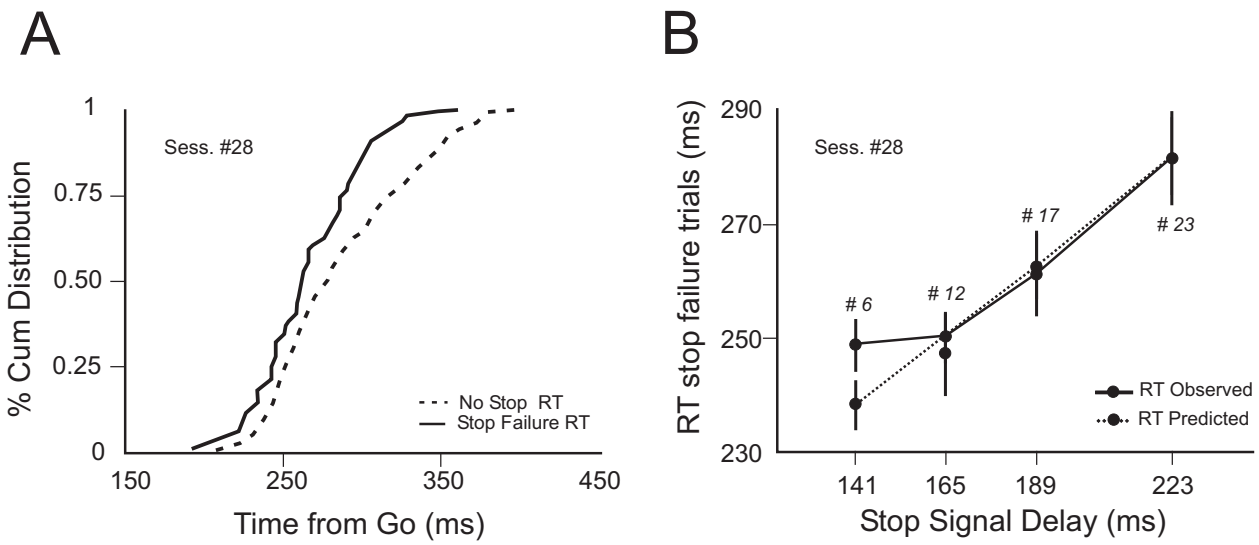

MIRABELLA ET AL., FIGURE 3

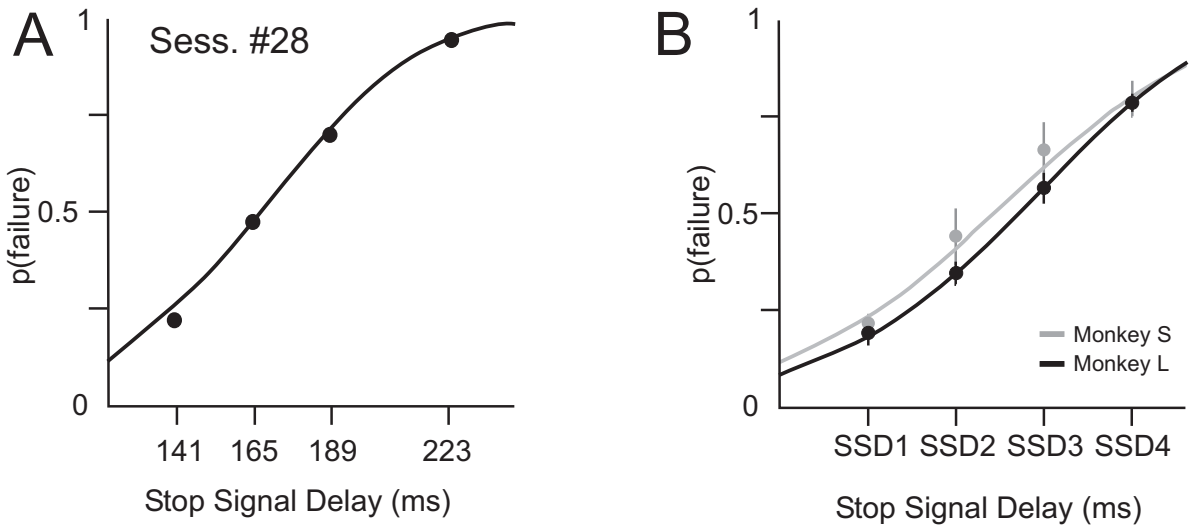

MIRABELLA ET AL., FIGURE 4

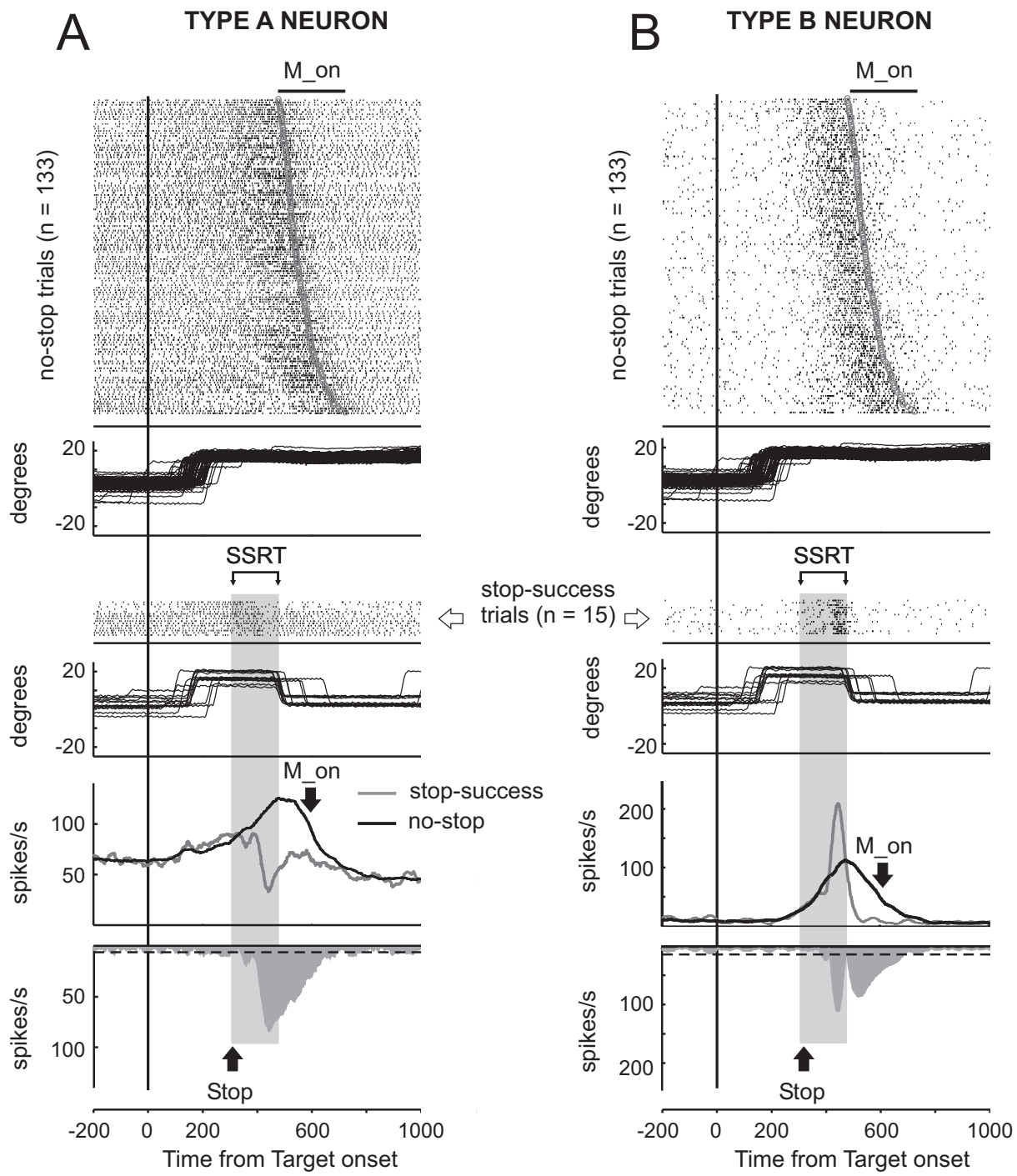

MIRABELLA ET AL., FIGURE 5

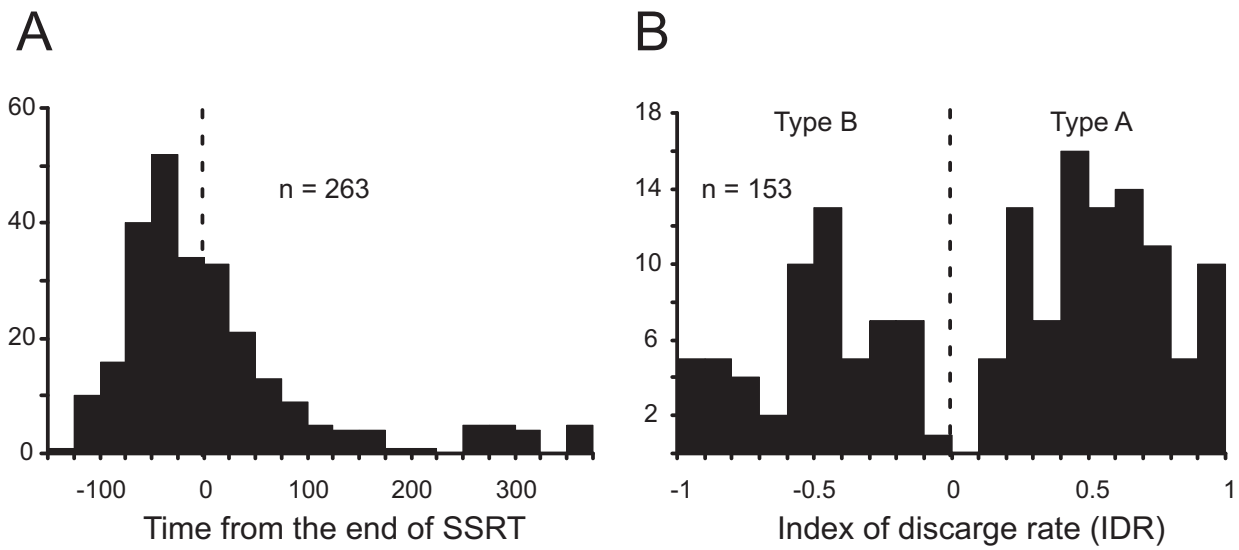

MIRABELLA ET AL., FIGURE 6

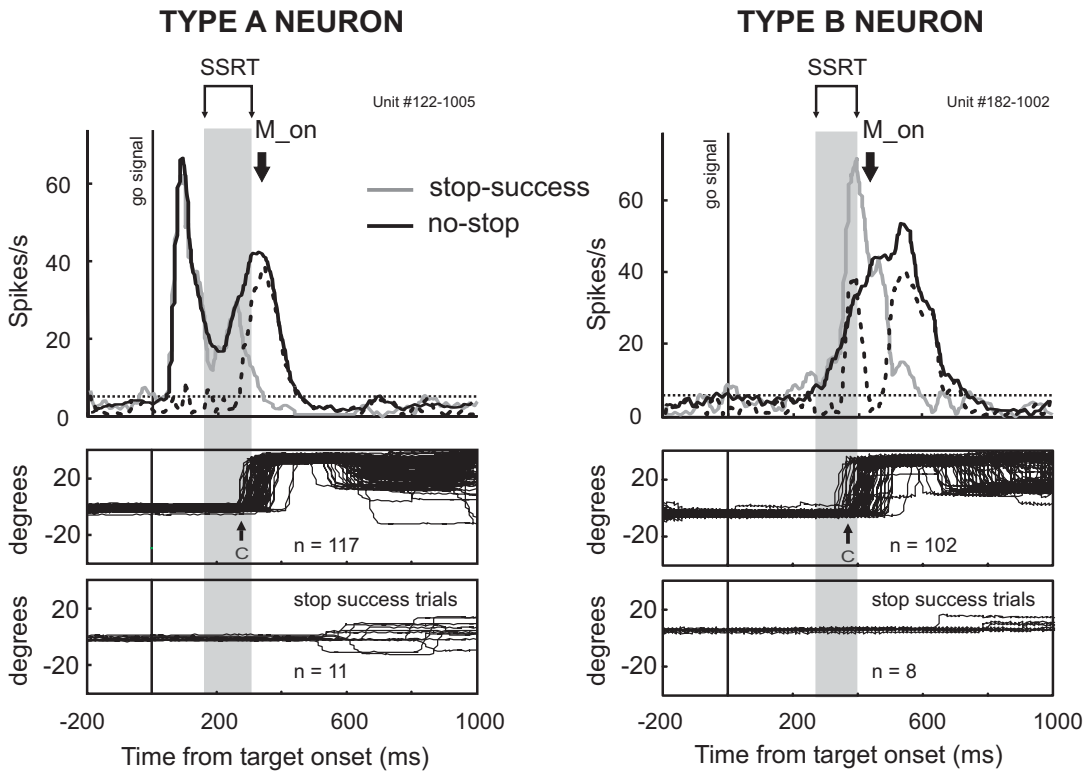

MIRABELLA ET AL., FIGURE 7

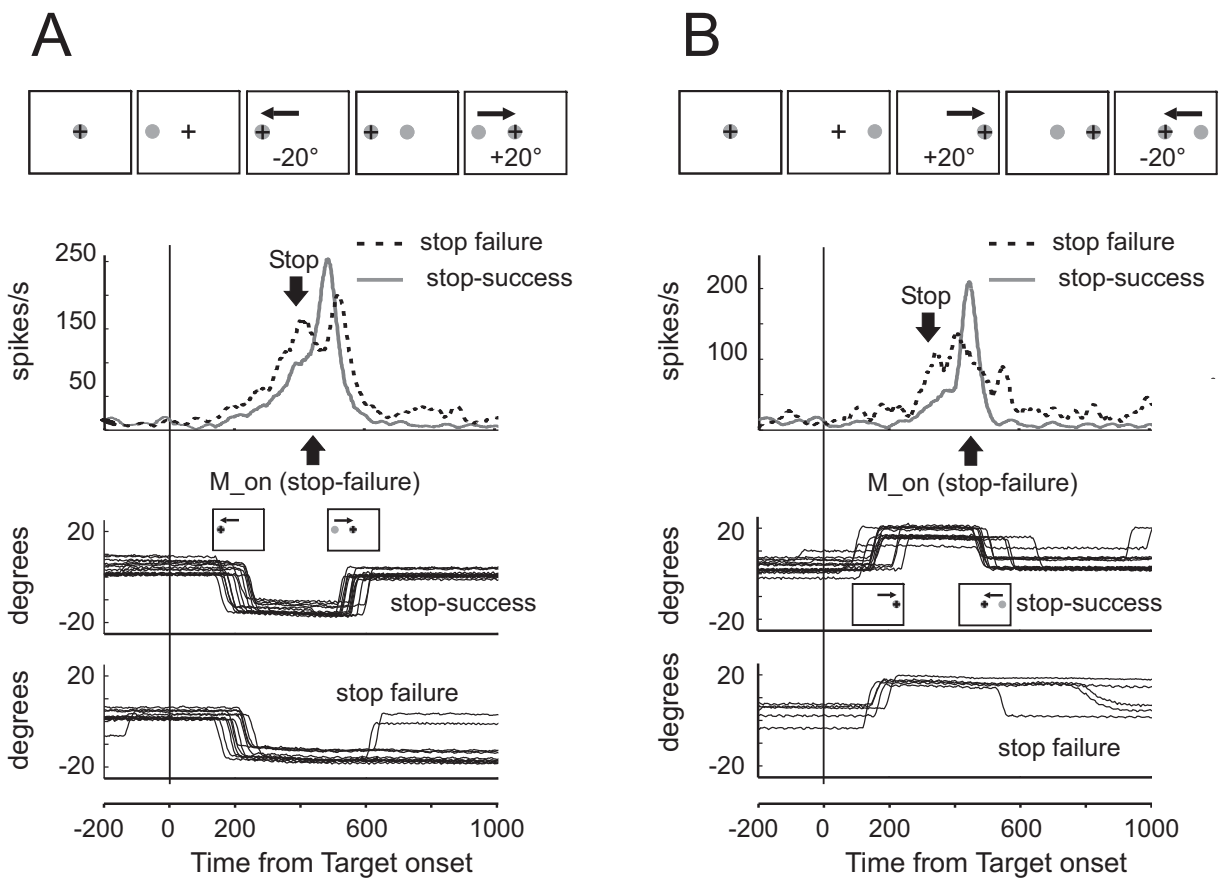

MIRABELLA ET AL., FIGURE 8

	Monkey L	Monkey S
FIXED SSDS		
RT no-stop success trials (ms)	361.6 ± 6.7	504.8 ± 15.2
MT no-stop success trials (ms)	170.5 ± 1.8	192.6 ± 7.6
RT no-stop-failure trials (ms)	338.2 ± 6.6	472.5 ± 15.5
Accuracy no-stop trials (%)	96.9 ± 0.7	97.1 ± 0.8
SSRT "integration method" (ms)	136.5 ± 1.7	157.3 ± 4.8
SSRT "random variable" (ms)	138.9 ± 2.9	163.8 ± 8.2
STAIRCASE		
RT no-stop success trials (ms)	-	508 ± 10.2
MT no-stop success trials (ms)	-	196.4 ± 5.2
RT no-stop-failure trials (ms)	-	474.9 ± 9.8
Accuracy no-stop trials (%)	-	95.2 ± 0.6
SSRT (ms)	-	147.5 ± 4.6
SSRT for SSDs presented > 20 times (ms)	-	147.5 ± 5.8
Representative SSD (ms)	-	351.9 ± 13.7
P(failure) (%)	-	48.4 ± 0.3

Table 1. Behavioral performance of arm movement for the two monkeys during the countermanding sessions. Accuracy is the percentage of no-stop trials correctly executed in the experimental block (see text for further details).

	Monkey L	Monkey S
Total SSD	292	174
SSD with computable divergence	228	160
SSD without divergence	97	27
SSD with divergence before SSRT	68	85
SSD with divergence after the SSRT	63	48

Table 2. Number of SSDs on which was compared the neural activity in stop-success versus latency matched no-stop trials in the two monkeys.